Modulating the Redox Potential of the Stable Electron Acceptor, Q(B), in Mutagenized Photosystem II Reaction Centers

ARTICLE *in* BIOCHEMISTRY · FEBRUARY 2011

Impact Factor: 3.02 · DOI: 10.1021/bi1017649 · Source: PubMed

2 AUTHORS, INCLUDING:

Richard T Sayre
Los Alamos National Laboratory and New M…

109 PUBLICATIONS **4,404** CITATIONS

SEE PROFILE

BIOCHEMISTRY
including biophysical chemistry & molecular biology
Article

Biochemistry **XXXX,** *XXX,* 000–000 A
DOI: 10.1021/bi1017649

Modulating the Redox Potential of the Stable Electron Acceptor, Q_B, in Mutagenized Photosystem II Reaction Centers[†]

Zoee Perrine[‡,§] and Richard Sayre*[,§]

[‡]*The Ohio State University Biophysics Program, Columbus, Ohio 43210, United States, and* [§]*The Donald Danforth Plant Science Center, St. Louis, Missouri 63132, United States*

Received November 3, 2010; Revised Manuscript Received January 14, 2011

ABSTRACT: One of the unique features of electron transfer processes in photosystem II (PSII) reaction centers (RC) is the exclusive transfer of electrons down only one of the two parallel cofactor branches. In contrast to the RC core polypeptides (psaA and psaB) of photosystem I (PSI), where electron transfer occurs down both parallel redox-active cofactor branches, there is greater protein−cofactor asymmetry between the PSII RC core polypeptides (D1 and D2). We have focused on the identification of protein−cofactor relationships that determine the branch along which primary charge separation occurs (P_{680}^+/pheophytin$^-$(Pheo)). We have previously shown that mutagenesis of the strong hydrogen-bonding residue, D1-E130, to less polar residues (D1-E130Q,H,L) shifted the midpoint potential of the $Pheo_{D1}/Pheo_{D1}^-$ couple to more negative values, reducing the quantum yield of primary charge separation. We did not observe, however, electron transfer down the inactive branch in D1-E130 mutants. The protein residue corresponding to D1-E130 on the inactive branch is D2-Q129 which presumably has a reduced hydrogen-bonding interaction with $Pheo_{D2}$ relative to the D1-E130 residue with $Pheo_{D1}$. Analysis of the recent 2.9 Å cyanobacterial PSII crystal structure indicated, however, that the D2-Q129 residue was too distant from the $Pheo_{D2}$ headgroup to serve as a possible hydrogen bond donor and directly impact its midpoint potential as well as potentially determine the directionality of electron transfer. Our objective was to characterize the function of this highly conserved inactive branch residue by replacing it with a nonconservative leucine or a conservative histidine residue. Measurements of Chl fluorescence decay kinetics and thermoluminescence studies indicate that the mutagenesis of D2-Q129 decreases the redox gap between Q_A and Q_B due to a lowering of the redox potential of Q_B. The resulting increased yield of $S_2Q_B^-$ charge recombination in the D2-Q129 mutants leads to an increased susceptibility to photoinhibitory light presumably due to $^3P_{680}$-mediated oxidative damage. The results indicate that the D2-Q129 residue plays a critical role in stabilizing the charge-separated state in PSII and further documents the structural and functional asymmetry between the two cofactor branches in PSII.

PSII[1] is a multisubunit pigment−protein complex that catalyzes the light-driven oxidation of water and reduction of plastoquinone (PQ) in oxygenic photoautotrophs. The structure of PSII from thermophilic cyanobacteria is now available at 2.9 Å resolution, along with several lower resolution crystal structures (3−3.8 Å) (*1*−*4*). PSII has two cofactor branches extending across the membrane which are related by a pseudo-*C*2 axis of symmetry. However, only one of these two branches participates in primary electron transfer and is referred to as the active branch.

It is well established that the primary electron acceptor in PSII is a Pheo molecule, $Pheo_{D1}$, which resides on the active branch (*5*−*11*). Similar to the bacterial reaction center (BRC), there is a symmetry-related Pheo ($Pheo_{D2}$) on the inactive branch of PSII (Figure 1). Prior to the availability of a high-resolution PSII crystal structure, the presence of a hydrogen-bonding interaction between the D1-130 residue and the ring V carbonyl group of $Pheo_{D1}$ was established using a combination of site-directed mutagenesis and spectroscopy (*7*, *12*). EPR studies of the D1-E130Q or H and D1-E130L mutations that were designed to weaken or abolish this hydrogen bond, respectively, in *Chlamydomonas* exhibited an upward shift in the g_x component of the Pheo anion radical *g* tensor consistent with a reduction of hydrogen-bonding strength to $Pheo_{D1}$ in the mutant PSII reaction centers (*7*). Further, Chl fluorescence decay kinetics and TL data obtained for the D1-E130L *Chlamydomonas* and D1-Q130L cyanobacterial mutants indicated that the loss of the hydrogen bond to $Pheo_{D1}$ was associated with a longer lifetime for $S_2Q_A^-$ charge recombination and an increased energetic gap between the primary radical pair, $P_{680}^+Pheo_{D1}^-$, and $P_{680}^+Q_A^-$ (*10*, *13*, *14*). It was determined that mutagenesis of D1-130 to amino acids that weakened the hydrogen-bonding interaction to $Pheo_{D1}$ shifted the midpoint potential of the $Pheo_{D1}/Pheo_{D1}^-$ couple to more negative values, lowering the probability of forming the primary radical pair and thus reducing the yield of the charge-separated state (*12*, *13*).

The function of $Pheo_{D2}$ and the potential effects of its protein environmental interactions on its possible function are less well understood than for $Pheo_{D1}$. Circular dichroism spectra of

[†]This work was supported by U.S. Air Force—Office of Scientific Research and U.S. Department of Energy, Center for Advanced Biofuel Systems.

*To whom correspondence should be addressed. Phone: 314-587-1437. Fax: 314-587-1537. E-mail: rsayre@danforthcenter.org.

[1]Abbreviations: BRC, purple bacterial reaction center; Chl, chlorophyll; DCMU, 3-(3,4-dichlorophenyl)-1,1-dimethylurea; ET, electron transfer; OEC, oxygen evolving complex; PBQ, *p*-benzoquinone; Pheo, pheophytin; PI, photoinhibitory; PQ, plastoquinone, PSII, photosystem II; Q_A, primary quinone electron acceptor; Q_B, secondary quinone electron acceptor; RC, reaction center; S_2, S_2 state of the oxygen evolving complex; TL, thermoluminescence.

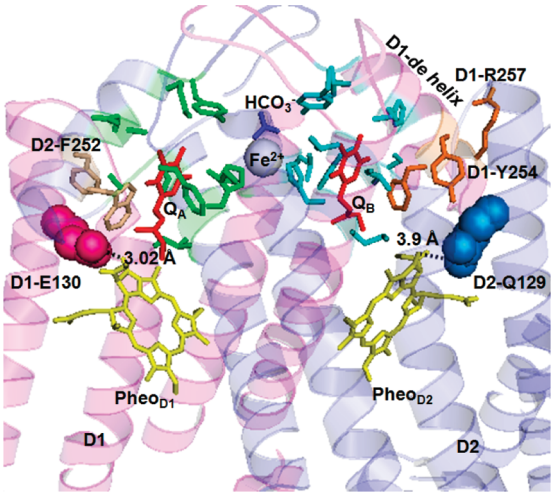

FIGURE 1: Structure of the acceptor side of photosystem II. This view of PSII is in an orientation parallel to the plane of the membrane and was created using PyMOL (2006 DeLano Scientific LLC) and the 3BZ1 cyanobacterial PSII crystal structure (*4*). Interatomic distances are indicated by dashed black lines. The amino residues forming the Q_A and Q_B binding pockets are shown in green and cyan, respectively. Amino acid residues of the D1-*de helix* that are known to play a role in determining the redox potential of Q_B are shown in orange, and the corresponding residues of the Q_A site are shown in pale brown.

isolated PSII RCs with selective pigment substitutions in the $Pheo_{D2}$ site have, however, provided evidence indicating that $Pheo_{D2}$ is excitonically coupled to the central multimeric RC chlorins (*15*, *16*) and is involved in excitation energy equilibration within the RC complex (*16*). The substitution of $Pheo_{D2}$ with a Chl molecule in the D1-L210H *Chlamydomonas* mutant has been shown to cause substantial impairment of PSII ET associated with drastically reduced oxygen evolution rates and charge separation yields (*16*). Consistent with the role of $Pheo_{D2}$ in energy transfer, circular dichroism spectra of D1-L210H RCs exhibited new excitonic interactions between the substituted Chl in the $Pheo_{D2}$ site and the neighboring pigments indicating that there was a redistribution of the excited state among the RC pigments, preventing charge separation on the active branch (*16*). These studies indicated that $Pheo_{D2}$ plays a critical role in ensuring proper distribution of excitation energy among pigments of the multimer complex such that efficient charge separation can take place on the active branch.

The inactive branch residue analogous to the D1-E130 residue which hydrogen bonds to $Pheo_{D1}$ in chloroplastic PSII RCs is the D2-Q129 residue. It has been suggested that this residue also hydrogen bonds to the headgroup of $Pheo_{D2}$ (*17*, *18*). However, analysis of the most recent PSII crystal structure from the cyanobacterium *Thermosynechococcus elongatus* at 2.9 Å resolution (*4*) reveals that the side chain of D2-Q129 is 3.9 Å away from the $Pheo_{D2}$ headgroup and therefore may not be in close enough proximity to serve as a hydrogen bond donor (Figure 1). A comparison of all 152 PSII D2 protein sequences available from a variety of oxygenic photoautotrophs shows that the D2-Q129 residue is completely conserved across all sequences, unlike the corresponding residue in the BRC (*19*).

In this work we employed site-directed mutagenesis to determine the role of the highly conserved acceptor side residue D2-Q129 in PSII. We substituted the D2-Q129 residue with a nonconservative hydrophobic leucine residue (D2-Q129L) or a conservative histidine residue (D2-Q129H). Our results demonstrate that mutagenesis of D2-Q129 to leucine and histidine leads to an acceleration and increased yield of $S_2Q_B^-$ charge recombination consistent with an effect of the D2-Q129 substitutions on the redox potential of Q_B which alters the stability of the charge-separated state in PSII.

MATERIALS AND METHODS

Generation of the D1-E130 and D2-Q129 Chlamydomonas Mutants. Site-directed mutations were introduced into the *Chlamydomonas reinhardtii psbA* (encodes the D1 PSII RC protein) and *psbD* (encodes the D2 PSII RC protein) genes using the Quik-Change site-directed mutagenesis kit from Stratagene. The pBA155 (*20*) and pBD202 (Minagawa, personal communication) vectors containing the *psbA* and *psbD* genes were used as the templates for site-directed mutagenesis. Both plasmids also contained the *aadA* gene that confers resistance to the antibiotics spectinomycin and streptomycin (*21*). A mutation was introduced at position 130 of the D1 protein in which the glutamate codon GAG was replaced with a leucine codon CTT using the CTACATGGGTCGACTTTGGGAATTATC forward and the complementary reverse primer to generate the D1-E130L plasmid. Similarly, two different point mutations were introduced at position 129 of the D2 protein. The glutamine-129 codon CAG was mutagenized either to CTG (leucine substitution) or to CAC (histidine substitution) using the GGTTTCATGCTTCGTCTG-TTTGAAATTGCTCGTTC and TTGGTTTCATGCTTCGT-CACTTTGAAATTGCTCGTTCAG forward primers and their complementary reverse primers to generate the D2-Q129L and D2-Q129H plasmids, respectively. The *psbA* mutation was confirmed by PCR and sequencing using the D1-5′UTR (GGA-CGTAGGTACATAAATGTGCTAGGTAAC) and D13′UTR (CCTGCCAACTGCCTATGGTAGCTATTAAGT) primers whereas the *psbD* mutations were confirmed using the D2-5′UTR (GTGATGACTATGCACAAAGCAGTTCTAGTCCC) and D2-3′UTR (CAAGCACTCATGTGATTTTTAGCCCCAAAG-GG) primers.

The D1-E130L plasmid was introduced into the *psbA* deletion strain CC-4147 (*Chlamydomonas* Center, Duke University) by particle gun bombardment to generate the D1-E130L mutant. The pBD202, D2-Q129L, and D2-Q129H vectors were transformed into a *psbD* deletion mutant, ΔD2-2-6 (Minagawa, personal communication) by particle bombardment to generate the complemented wild-type (WT) and D2-Q129L and D2-Q129H mutant strains, respectively. The D1-E130L and D2-Q129L plasmids were also cotransformed into a {Δ*psbA*, Δ*psbD*} double deletion strain (*22*) to generate the D1-E130L/D2-Q129L double mutant with substitutions at positions 130 and 129 of the D1 and D2 proteins, respectively, to leucine.

Following bombardment, the cells were plated on Tris−acetate−phosphate (TAP) medium (*23*) containing 100 μg/mL spectinomycin and incubated at 22 °C under dim light. Putative transformants were selected on the basis of spectinomycin and streptomycin resistance. DNA extracted from the transgenics via the Chelex-100 extraction method (*24*) was used as template for DNA sequence confirmation of the mutagenized *psbA* and *psbD* genes using PCR primers D1-5′/3′UTR and D2-5′/3′UTR.

Growth Conditions. All strains were maintained on TAP agar plates containing 100 μg/mL spectinomycin and 50 μg/mL ampicillin and were grown in liquid TAP media without antibiotics to mid log phase or until the optical density of the culture at 750 nm reached 0.8−1.0, for subsequent measurements. The complemented wild-type (WT) and mutant strains were normalized on the basis of cell number and assayed for photoautotrophic

growth on high salt (HS) media (*25*) under low light conditions (~30 μmol of photons m^{-2} s^{-1}). In addition, the WT, D2-Q129L, and D2-Q129H mutants were also grown in photoautotrophic growth media under high light conditions (~500 μmol of photons m^{-2} s^{-1}).

Rates of Oxygen Evolution. Oxygen evolution activity of wild-type and mutant cells was measured under saturating conditions of ~850 of μmol photons m^{-2} s^{-1} of 650 nm light, using a Clark-type oxygen electrode (Hansatech Instruments, Norfolk, England) as described previously (*26*). The Chl concentration of the sample was ~10 μg of Chl/mL.

Flash-Induced Chl Fluorescence Induction and Decay. Chl *a* fluorescence induction transients of wild-type and mutant cells were measured with a pulse-modulated fluorometer (FL 3500; Photon Systems Instruments, Brno, Czech Republic). Before the measurements the cells were resuspended in TAP medium at a Chl concentration of 5 μg/mL and dark adapted for 10 min.

Chl *a* fluorescence decay following a single turnover saturating flash was assayed in whole cells in the presence or absence of 20 μM DCMU at a Chl concentration of 5 μg/mL. The Chl fluorescence decay curves measured in the absence of DCMU were fit using three lifetime components: a fast and intermediate exponential component and a slow hyperbolic component as described previously (*27*). When measured in the presence of DCMU, the fitting function included only two components, fast and slow phases representing Q_A^- recombination with $Tyr_Z^\bullet$ and S_2, respectively.

Thermoluminescence Measurements. TL from whole cells was measured in the presence and absence of 20 μM DCMU using a thermoluminescence instrument manufactured by Photon Systems Instruments, Brno, Czech Republic. A cell suspension of 50 μg of Chl per 50 μL in 20 mM HEPES at pH 7.5 and 0.5 μM nigericin was spotted on a $^1/_2$ in. disk prepared from Whatman filter paper 1. The sample was dark adapted for 2 min and then cooled to 0 °C or −10 °C when TL was measured in the absence and presence of 20 μM DCMU, respectively. After 2 min, a single saturating flash was fired, and TL was recorded upon heating the sample at a rate of 0.5 °C/s. For PBQ treatment, cells were incubated with 100 μM PBQ for 10 min in the dark, then spun down, and washed to remove the residual PBQ before measurement.

Photoinhibition Measurements. *C. reinhardtii* cultures were grown as described above and resuspended in buffer A containing 0.35 M sucrose, 20 mM HEPES, pH 7.5, and 2 mM $MgCl_2$ to yield a Chl concentration of 1 mg of Chl/mL. Cells were then broken by sonication (Biologics, Inc., Model 300 V/T ultrasonic homogenizer) two times for 10 s each time (pulse mode, 50% duty cycle, output power 5) on ice. Unbroken cells were pelleted by centrifugation at 3200*g* for 1 min and the thylakoid membranes harvested by centrifugation of the supernatant obtained from the previous step at 12000*g* for 12 min. The membranes were then resuspended in fresh buffer at > 1.0 mg of Chl/mL. All steps were carried out in darkness at 4 °C. Isolated thylakoids at a Chl concentration of ~10 μg/mL were exposed to PI light (800 μmol of photons m^{-2} s^{-2}, 650 nm at 22 °C) and assayed for residual rates of oxygen evolution in the presence of 20 μM 2,5-dimethyl-1,4-benzoquinone (DMBQ), 2 mM potassium ferricyanide, and 30 mM methylamine.

RESULTS

Photoautotrophic Growth and Oxygen Evolving Activities of WT and D2-Q129L, D2-Q129H, D1-E130L, and D1-E130L/D2-Q129L Mutant Cells. As previously discussed, the

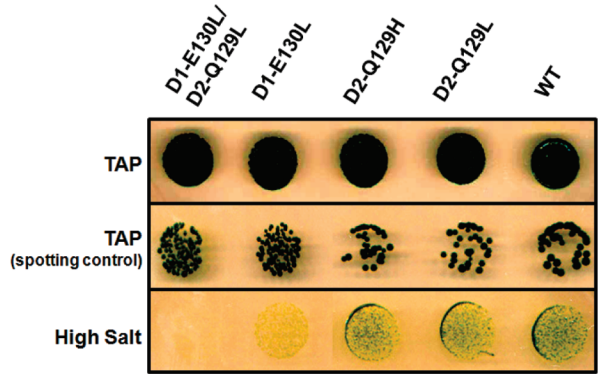

FIGURE 2: Comparative growth of the WT and mutant cells on TAP (photoheterotrophic) and high salt (photoautotrophic) media. The WT and mutants were plated at the same cell densities and grown for a period of 2 weeks under ~30 μE m^{-2} s^{-1} light.

D1-E130 residue is hydrogen bonded to the primary electron acceptor, $Pheo_{D1}$. The analogous inactive branch residue, D2-Q129, is conserved in oxygenic photosynthesis but is not in close enough proximity to the $Pheo_{D2}$ headgroup to have an analogous hydrogen-bonding interaction (*4*). In order to gain greater insight into the functional role of the D2-Q129 residue, we carried out site-directed mutagenesis to generate the D2-Q129L nonconservative and D2-Q129H conservative mutants. In addition, we generated D1-E130L single and D1-E130L/D2-Q129L double mutants to determine the impact of D2-Q129 mutations on charge transfer in a mutant (D1-E130L) background incapable of primary charge separation on the active branch. Preliminary photoautotrophic growth analyses of the D2-Q129L and D2-Q129H single mutants indicated that their growth was comparable to WT when grown at low light intensities (Figure 2). As expected, the D1-E130L and D1-E130L/D2-Q129L mutant strains grew very poorly under photoautotrophic growth conditions due to an impairment in charge separation.

To determine the effects of the D2-Q129 mutations on photosynthetic oxygen evolution, steady-state rates of oxygen evolution were measured at saturating light intensities. The light-saturated rates of oxygen evolution in the D2-Q129L and D2-Q129H mutants were ~70% and 90% of WT, respectively (Table 1). As expected, the oxygen evolving abilities of the D1-E130L and D1-E130L/D2-Q129L mutants were severely reduced, being only ~20% and 10% of WT rates, respectively. In general, the extent of photoautotrophic growth in the mutants correlated well with their oxygen evolving capacities.

Flash-Induced Chl Fluorescence Relaxation Kinetics. Figure 3 shows the flash-induced Chl fluorescence decay transients obtained for WT and mutant cells in the absence and presence of DCMU. In the WT, the fast and intermediate decay components obtained in the absence of DCMU contribute to ~90% of the total fluorescence decay representing forward ET from Q_A^- to Q_B when PQ is either present or absent from the Q_B site at the time of the flash (Table 2). The fast component, which is ~72% of the total decay, has a lifetime of ~0.29 ms in WT *Chlamydomonas* cells and arises from the reoxidation of Q_A^- by PQ molecules bound to the Q_B site, which were either in the oxidized or in the semireduced state, before the flash. Since the ratio of Q_B to Q_B^- in undisrupted cells is 1 (*28*), the fast lifetime component represents an approximately equal contribution of the Q_A^- to Q_B and Q_A^- to Q_B^- electron transfer steps. The mean lifetime of the fast component was relatively unaltered in the D2-Q129L and D2-Q129H mutants, being ~0.26 and 0.29 ms,

Table 1: Rates of Steady-State Oxygen Evolution Measured in TAP Medium Using Whole Cells of the Complemented WT and Mutants as Shown[a]

strain	oxygen evolved (μmol of O_2 (mg of Chl)$^{-1}$ h^{-1})	% WT
WT	113 ± 3.0	100
D2-Q129L	78 ± 2.6	69
D2-Q129H	101 ± 4.4	89
D1-E130L	25 ± 1.3	22
D1-E130L/D2-Q129L	10 ± 2.0	9

[a]Standard errors of the rates are indicated and were calculated for six to nine individual measurements from at least three independent cultures.

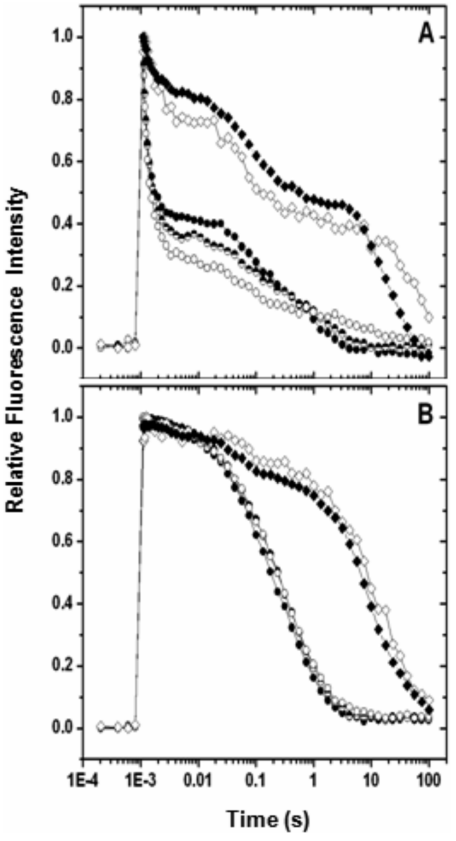

FIGURE 3: Flash-induced Chl fluorescence decay kinetics measured in WT and mutant cells in the absence (A) and presence (B) of 20 μM DCMU. WT (open circles), D2-Q129L (closed circles), D2-Q129H (semiclosed circles), D1-E130L (open diamonds), and D1-E130L/D2-Q129L (closed diamonds) were excited with a single turnover saturating flash at 1 ms. The curves are shown after normalization to the $F_m - F_0$ value for each strain.

respectively. The intermediate lifetime component in the D2-Q129 mutants was also similar to the WT at ~35 ms. However, the total contribution of forward ET to the overall Chl fluorescence decay measured as the sum of the relative amplitudes of the fast and intermediate lifetime components was significantly reduced in the D2-Q129L and D2-Q129H mutants relative to WT. Conversely, the contribution of the slow component, which represents charge recombination between S_2 and Q_B^-, showed an ~2−3-fold increase in the D2-Q129H and D2-Q129L mutants compared to WT, and its lifetime was accelerated ~4−6-fold from ~3.3 s in WT to 0.54 and 0.73 s in the D2-Q129L and H mutants, respectively (Table 2). These data indicated that mutagenesis of the D2-Q129 residue did not impact the forward rate of ET but caused an acceleration of $S_2Q_B^-$ charge recombination. Moreover, the probability of forward ET decreased in the D2-Q129L and D2-Q129H mutants while the probability of $S_2Q_B^-$ charge recombination increased, indicating a decrease in the overall activation energy for $S_2Q_B^-$ charge recombination in the D2-Q129 mutants relative to WT.

Given the proximity of the D2-Q129 residue to the inactive cofactor branch of PSII, we thought it necessary to ascertain whether $S_2Q_B^-$ charge recombination in the D2-Q129 mutants occurred via active or inactive branch cofactors. In order to do this, we generated the D1-E130L/D2-Q129L double mutant in which the protein environment associated with both active and inactive branch cofactors was altered. A manifestation of the combined effects of the D1-E130L and D2-Q129L mutations in the double mutant on $S_2Q_B^-$ charge recombination would suggest the involvement of active branch cofactors in charge recombination in the D2-Q129 mutants. As previously shown, the rate of forward ET in the D1-E130L single mutant was slower and its relative contribution reduced relative to WT (*14*). The lifetime of the fast component representative of forward ET from Q_A^- to Q_B was 0.77 ms in the mutant (0.29 ms in WT) while its relative amplitude decreased to 23% (72% in WT) (Table 2). This was indicative of an impairment of forward ET in the D1-E130L mutant which corroborated the poor photoautotrophic growth and oxygen evolution rates. Similarly, the slow component of the Chl fluorescence decay representative of $S_2Q_B^-$ charge recombination was also substantially slower in the mutant with a lifetime of ~100 s compared to only 3.3 s in WT but had a larger contribution (~50%) to the overall Chl fluorescence decay. This increase in lifetime and yield of $S_2Q_B^-$ recombination was attributed to an increased energetic gap between $P_{680}^+Pheo_{D1}^-$ and $P_{680}^+Q_A^-$ (Q_B^-), due to a change in the free energy of the primary radical pair $P_{680}^+Pheo_{D1}^-$ to more negative values compared to WT (*10*, *13*, *14*). The D1-E130L/D2-Q129L double mutant, which combines the effects of the D1-E130L and D2-Q129L single mutations, had a decreased yield for forward ET from Q_A^- to Q_B that contributed to ~18% of the overall Chl fluorescence decay, compared with 72% in WT. However, the double mutant had a faster back-reaction that contributed to ~58% of the total decay compared to ~48% in the D1-E130L background strain (Table 2). Hence, the mutagenesis of D2-Q129 in the D1-E130L mutant background led to an increased yield of $S_2Q_B^-$ charge recombination, similar to the D2-Q129 single mutants.

Flash-Induced Chl Fluorescence Decay in the Presence of Q_B-Site Inhibitors. To determine whether the D2-Q129 mutations also affected charge recombination between the S_2 state of the OEC and Q_A^-, we monitored the decay of Chl fluorescence in the presence of a Q_B site inhibitor, DCMU. DCMU binds to the Q_B binding site blocking forward ET from Q_A^- to Q_B. Under these conditions, the reoxidation of Q_A^- occurs via back-reactions with donor side components including the S_2 state of the OEC ($S_2Q_A^-$ charge recombination). Analyzing Chl fluorescence decay kinetics in the presence of DCMU also yields information about changes in the midpoint potentials of cofactors that are energetically between the OEC and Q_A in the ET chain. Chl fluorescence transients measured in the presence of DCMU revealed no significant kinetic differences in the D2-Q129L and D2-Q129H mutants relative to WT (Figure 3B, Table 2). The slow decay component representative of $S_2Q_A^-$ recombination had a mean lifetime of ~0.26 s in the WT and ~0.23 and 0.27 s in the D2-Q129L and D2-Q129H mutants, respectively (Table 2). These results implied that D2-Q129 mutagenesis had no impact on the energetic gap between S_2

Table 2: Lifetimes and Relative Amplitudes of the Different Chl Fluorescence Decay Components of WT and Mutants Shown in Figure 3[a]

	forward ET		charge recombination
strain	fast T_1 (ms)/Amp (%)	intermediate T_2 (ms)/Amp (%)	slow T_3 (s)/Amp (%)
no addition			
WT	0.29 ± 0.02/72 ± 3	34.4 ± 19.6/17 ± 2	3.3 ± 1.07/11 ± 1
D2-Q129L	0.26 ± 0.02/62 ± 2	34.3 ± 15.5/11 ± 1	0.54 ± 0.07/28 ± 2
D2-Q129H	0.29 ± 0.02/66 ± 2	32.4 ± 15.1/11 ± 1	0.73 ± 0.15/23 ± 2
D1-E130L	0.77 ± 0.91/23 ± 1	98.7 ± 5.3/29 ± 2	98.8 ± 11/48 ± 4
D1-E130L D2-Q129L	0.51 ± 0.15/18 ± 2	93.5 ± 18.3/24 ± 1	28.1 ± 3.4/58 ± 2
DCMU			
WT	5.4 ± 2.2/5.4 ± 0.72		0.26 ± 0.01/94.7 ± 0.72
D2-Q129L	8.7 ± 1.6/7.3 ± 1.3		0.23 ± 0.04/92.7 ± 1.3
D2-Q129H	12.6 ± 3.7/7.0 ± 0.9		0.27 ± 0.02/93.0 ± 0.9
D1-E130L	72.9 ± 32.9/9.8 ± 0.7		10.3 ± 1.6/90.2 ± 0.7
D1-E130L D2-Q129L	26.4 ± 12.0/15.9 ± 1.4		11.4 ± 2.0/84.1 ± 1.4

[a]The standard deviations are indicated and were obtained from multiple measurements (n = 9).

and Q_A^- or on the energetics of any of the intermediate redox cofactors on the active branch.

It is well documented that the midpoint potential of $Pheo_{D1}$ and the free energy of the $P_{680}^+Pheo_{D1}^-$ radical pair is decreased in the D1-E130L mutant due to the elimination of the hydrogen-bonding interaction to the $Pheo_{D1(active)}$ headgroup (*10*, *13*). Unlike the case of the D2-Q129 mutations where $S_2Q_A^-$ charge recombination was unaffected, the D1-E130L mutation induced a slowing of $S_2Q_A^-$ charge recombination (*10*, *13*). The lifetime of the slow component representative of $S_2Q_A^-$ charge recombination in the D1-E130L mutant obtained from the Chl fluorescence decay transient in the presence of DCMU was ~10 s as compared to ~0.26 s in WT. This was expected as the mutagenesis of D1-E130L affects the midpoint potential of an ET cofactor ($Pheo_{D1}$) upstream of Q_B. As discussed above, mutagenesis of the D2-Q129 residue to leucine or histidine in the D2-Q129L and D2-Q129H single mutants did not alter $S_2Q_A^-$ recombination. As expected, the Chl fluorescence decay kinetics of the D1-E130L/D2-Q129L double mutant measured in the presence of DCMU showed no significant differences from the D1-E130L mutant. The mean lifetime of the slow component in the D1-E130L/D2-Q129L mutant was ~11 s, compared to ~10 s in D1-E130L (Table 2).

It is clear that mutations of the D2-Q129 residue impact the kinetics of Chl fluorescence decay only in the absence of Q_B site inhibitors, suggesting the involvement of Q_B in the changes observed in the D2-Q129 mutants compared to WT. More specifically, while the rates of forward ET from Q_A^- to Q_B and $S_2Q_A^-$ charge recombination are unchanged in the D2-Q129L and D2-Q129H mutants, the rate of $S_2Q_B^-$ charge recombination is accelerated 4−6-fold in the mutants relative to WT. This confirms that mutagenesis of the D2-Q129 residue to leucine or histidine affects Q_B while not impacting other active branch cofactors. Moreover, comparative analyses of Chl fluorescence decay kinetics in the presence and absence of DCMU suggest that mutagenesis of the D2-Q129 residue induced a decrease in the free energy of the $S_2Q_B^-$ charge pair and in the energetic gap between Q_A and Q_B.

Chl Fluorescence Induction Kinetics. To obtain further information on ET involving the acceptor side of PSII, Chl *a* fluorescence induction kinetics were measured under continuous illumination in WT and mutant strains for up to 1 s (*29*). Figure 4 shows the Chl fluorescence induction transients plotted on a logarithmic time scale. The first phase of the fluorescence rise kinetics, labeled I, reflects the reduction of Q_A to Q_A^- (*30*, *31*). The rise to P is attributed to reduction of the plastoquinone pool. As shown in Figure 4, the Chl fluorescence induction kinetics in the D2-Q129 mutants were similar to WT for the I and P phases. However, the relative intensity of the I phase measured at 8 ms after the start of the illumination increased from 0.39 in WT to 0.46 and 0.53 in the D2-Q129L and D2-Q129H mutants, respectively. This result indicated an increase in the level of Q_A^-, consistent with a change in the equilibrium of the reaction $Q_A^-Q_B \leftrightarrow Q_AQ_B^-$ toward Q_A^- or an increased number of non-Q_B centers in the mutants (*32*). Noticeably, and consistent with the effects of the D2-Q129L mutation, the amplitude of the I phase was significantly larger in the D1-E130L/D2-Q129L mutant with a relative intensity of 0.74 compared to 0.65 in the D1-E130L mutant also indicating a shift in the equilibrium of $Q_A^-Q_B \leftrightarrow Q_AQ_B^-$ toward Q_A^-.

TL Properties Measured in the Absence and Presence of 20 μM DCMU. TL is the temperature-dependent emission of light from PSII resulting from recombination of stabilized charge-separated pairs formed following excitation. Warming of the stabilized (frozen) charge-separated state increases the vibrational energy of the donor and acceptor allowing for the recombination of charge-separated pairs with re-formation of the P_{680}* high energy state. P_{680}* then decays back to the ground state with the emission of a photon (TL) (*33*−*36*). The peak position and shape of a TL band are determined by the free energy of activation required for radiative recombination of a particular charge transfer pair. Hence, the properties of TL bands are extremely sensitive to the energetic gaps between donors and acceptors, which in turn are dependent on redox potentials of the recombination partners. In PSII, a significant proportion of charge recombination reactions proceed via nonradiative pathways which also play an important role in determining TL yield (*10*, *14*).

In the absence of Q_B site ET inhibitors such as DCMU, the TL band generated from WT *Chlamydomonas* cells arises due to charge recombination between the Q_B^- and S_2 radical pair and has a maximum emission at 28 °C (Figure 5A). This is commonly referred to as the B band (*33*, *36*). The peak temperature of the B band decreased to ~10 and 15 °C in the D2-Q129L and D2-Q129H mutants, respectively. This observation was consistent with results obtained from the flash-induced Chl fluorescence decay kinetics which revealed an acceleration of $S_2Q_B^-$ charge recombination in the D2-Q129 mutants relative to WT. In contrast, in the D1-E130L mutant, the B band was ~10 times

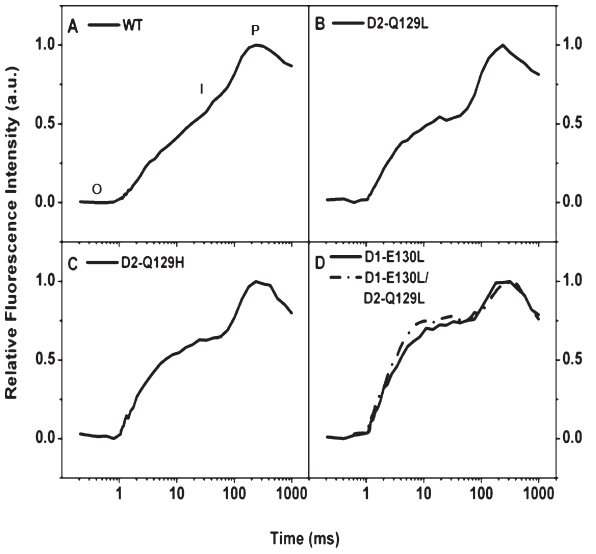

FIGURE 4: Chl *a* fluorescence induction transients of *C. reinhardtii* WT and mutant cells. Cells from the (A) WT, (B) D2-Q129L, (C) D2-Q129H, (D) D1-E130L (solid line), and D1-E130L/D2-Q129L double mutant (dot and dash line) were grown mixotrophically and normalized for Chl concentration. The data are plotted on a logarithmic time scale and shown after normalization to the $F_m - F_0$ value for each strain.

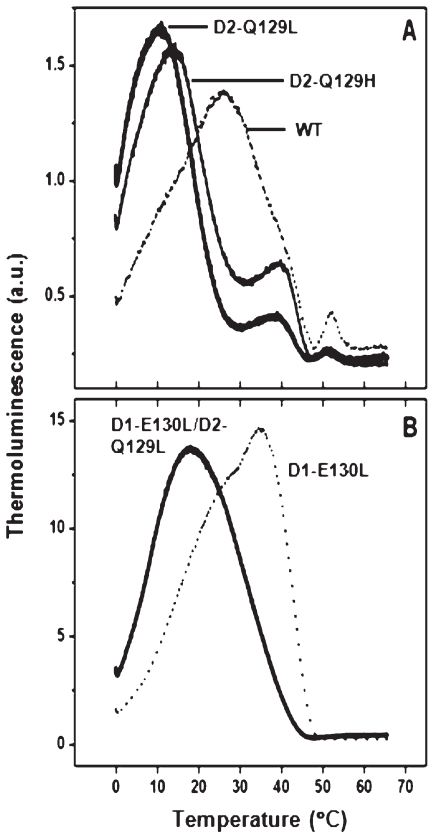

FIGURE 5: TL characteristics of the WT and mutants in the absence of ET inhibitors. WT and the D2-Q129L and D2-Q129H mutants are shown in panel A, and the D1-E130L and D1-E130L/D2-Q129L mutants are shown in panel B. TL was excited with a single turnover saturating flash at 0 °C and measured using a 0.5 °C/s heating rate.

more intense than in WT, with a higher peak temperature of ~36 °C (Figure 5B). This result was consistent with previous TL studies where the D1−130 residue in PSII was mutated to leucine (*14*). However, when the D1-E130L mutation was combined with the D2-Q129L mutation in the D1-E130L/D2-Q129L double mutant, the peak temperature of the B band decreased from ~36 °C in D1-E130L to ~18 °C in the double mutant. The D1-E130L/D2-Q129L double mutant manifested the combined effects of the two single mutations, indicating that the acceleration of $S_2Q_B^-$ charge recombination, induced by the D2-Q129 mutation, involved the active branch and not the inactive branch cofactors. Interestingly, the decrease of ~18 °C in B band peak temperature of the D1-E130L/D2-Q129L double mutant when compared to the D1-E130L single mutant background was comparable to the decrease of ~18 °C in the peak temperature of the B band in the D2-Q129L single mutant. The decreases in B band peak temperatures induced by mutations of the D2-Q129 residue are indicative of a decrease in the overall stability of the $S_2Q_B^-$ charge pair attributed to a change in the redox properties of the S_2 state of the OEC or of Q_B. Considering that the position of the D2-Q129 residue is far removed from the OEC, the more likely explanation is that D2-Q129 mutagenesis affects the redox properties of Q_B.

The TL data obtained for the WT and mutants in the presence of DCMU are shown in Figure 6. Under these conditions the B band is replaced by the Q-band which is representative of recombination between the $S_2Q_A^-$ charge pair (*33*, *36*) and has a peak emission at ~7 °C in WT (Figure 6A). The peak temperature of the Q-band observed in the D2-Q129L and D2-Q129H mutants was indistinguishable from WT, indicating that the overall stability of the $S_2Q_A^-$ charge pair and the stabilization of the S_2 state were not affected by mutagenesis of the D2-Q129 residue. This finding also confirmed that modification of the B band in the D2-Q129L and D2-Q129H mutants relative to WT and the D1-E130L/D2-Q129L double mutant relative to D1-E130L occurred due to alterations in the redox potential of Q_B and not due to changes in the redox properties of the S_2 state or any of the other redox components of the active branch. Although no changes were apparent in the peak temperature of the Q-band in the D2-Q129 mutants, an increase in Q-band intensity was consistently observed. The addition of DCMU to PSII centers that contain PQ in the semireduced state bound to the Q_B site results in the formation of Q_A^- prior to illumination (*37*). These centers are therefore not available for charge separation. The destabilization of the Q_B^- state in the D2-Q129 mutants presumably results in a lower concentration of stable Q_B^- in dark-adapted samples compared to wild type and translates to a decrease in $S_1Q_A^-$ formation on DCMU binding. This leads to a greater yield of $S_2Q_A^-$ formation upon illumination. Thus, the increase in Q-band intensity in the D2-Q129 mutants is indicative of the destabilization of Q_B^- in the mutants relative to wild type.

Figure 6B shows the Q-band obtained in the D1-E130L and D1-E130L/D2-Q129L mutants in the presence of DCMU. The change in primary radical pair energetics and increased free energy gap between $P_{680}^+Pheo_{D1}^-$ and $P_{680}^+Q_A^-$ was reflected by an increase in peak temperature of the Q-band in D1-E130L which occurred at ~25 °C when compared to 6−7 °C in WT, consistent with previous findings (*10*). When the D2-Q129L mutation was combined with the D1-E130L mutation in the D1-E130L/D2-Q129L strain, no changes were observed in the peak temperature of the Q-band. These results indicated that the D2-Q129L mutation did not induce a change in the free energy of the $S_2Q_A^-$ charge pair in the double mutant when compared to the D1-E130L single mutant background.

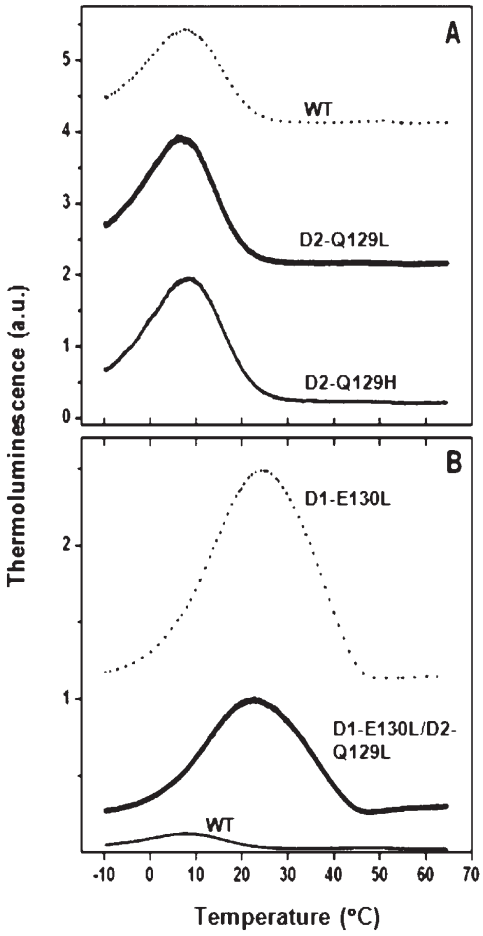

FIGURE 6: TL characteristics of the WT and mutants in the presence of 20 μM DCMU. WT and the D2-Q129L and D2-Q129H mutants are shown in panel A, and the D1-E130L and D1-E130L/D2-Q129L mutants are shown in panel B. TL was excited with a single turnover saturating flash at −10 °C and measured using a 0.5 °C/s heating rate.

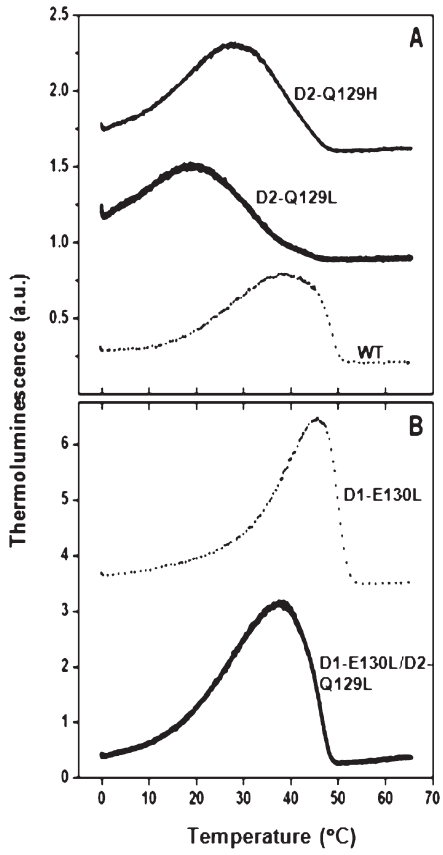

FIGURE 7: TL measured in WT and mutant cells after treatment with PBQ. WT and the D2-Q129L and D2-Q129H mutants are shown in panel A, and the D1-E130L and D1-E130L/D2-Q129L mutants are shown in panel B. TL was excited with a single turnover saturating flash at 0 °C and measured using a 0.5 °C/s heating rate.

The effect of the D2-Q129 mutations on TL properties of the B band and lack of effects on the Q-band corroborate the Chl fluorescence decay kinetics results. Taken together, these data demonstrate that mutagenesis of D2-Q129 decreases the stability of the $S_2Q_B^-$ charge-separated pair without impacting the energetics of the $S_2Q_A^-$ state. Hence, the differences in TL and Chl fluorescence decay kinetics of the D2-Q129 mutants relative to WT in the absence of Q_B site inhibitors are due to changes in the redox properties of Q_B and not due to energetic changes in any of the active branch ET cofactors between the OEC and Q_A in PSII.

Effect of p-Benzoquinone (PBQ) on $S_2Q_B^-$ Charge Recombination. To eliminate the possibility that the major TL band observed in the absence of DCMU in the D2-Q129 mutants arose due to the recombination of S_2 with Q_A^- rather than Q_B^-, we treated cells with 100 μM PBQ to oxidize the plastoquinone pool and minimize the possible contribution of Q_A^- to charge recombination (*10*, *38*). Under our conditions, the peak temperature of the B band obtained for the PBQ-treated WT cells was ~38 °C and was attributed to charge recombination between the $S_{2/3}$ states of the OEC and Q_B^- (*39*). After PBQ treatment, the peak temperature of the B band in the D2-Q129L and D2-Q129H mutants was 20 and 25 °C, respectively, indicating a destabilization of the $S_2Q_B^-$ state relative to WT (Figure 7A). A higher B band peak temperature was expected in the D1-E130L mutant due to an increase in the overall energetic gap between $P_{680}^+Pheo_{D1}^-$ and $P_{680}^+Q_A^-$ and was observed at ~46 °C relative to ~38 °C in WT after PBQ treatment. The introduction of a point mutation at D2-Q129 in the D1-E130L background as in the D1-E130L/D2-Q129L double mutant decreased the peak temperature of the TL band from ~46 °C in the D1-E130L mutant to ~36 °C in the double mutant (Figure 7B). Our main purpose for treating the samples with PBQ prior to the TL measurement was to oxidize the plastoquinone pool such that the contribution of Q_A^- to the TL signal (in the absence of DCMU) was minimal. However, PBQ is known to have other effects such as causing the transmembrane electrical potential to collapse and increasing the lifetime for charge recombination in PSII (*13*). Both of these effects of PBQ treatment are observed in all the strains tested here where the peak temperature of the B band, which dominates the TL signal in the absence of DCMU, is increased when compared to TL measured in the non-PBQ-treated cells.

Effects of Photoinhibitory (PI) Light Treatment. Based on analysis of the Chl fluorescence decay and TL measurements, it was seen that mutations of the D2-Q129 residue decreased the stability of the $S_2Q_B^-$ charge pair and consequently caused an increase in the probability of $S_2Q_B^-$ charge recombination. It is known that charge recombination reactions in PSII invariably induce photooxidative damage due to triplet Chl-mediated $^1O_2$ generation (*40*, *41*). The decrease in the midpoint potential of the Q_B/Q_B^- redox couple and the consequent decrease in the redox gap between Q_A and Q_B in the D2-Q129 mutants would be expected to increase the level of reduced Q_A. Lowering the redox gap between Q_A and Q_B is a well-acknowledged cold-stress (high light intensity) response intended to maintain the oxidized form

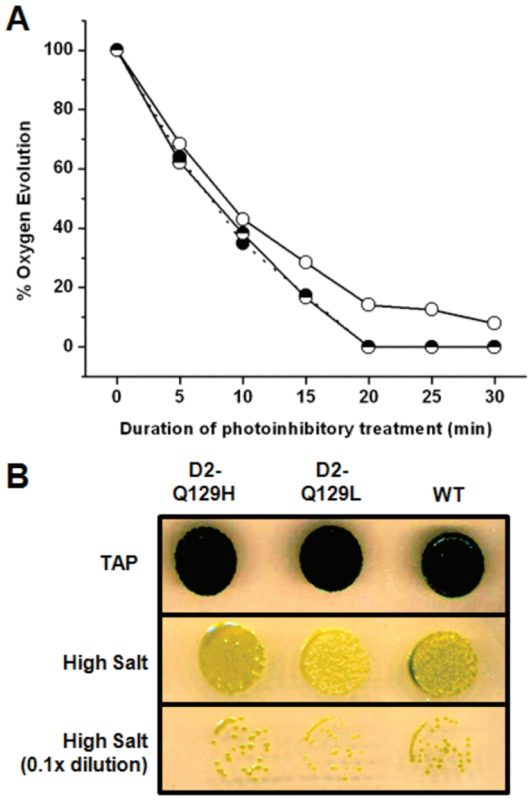

FIGURE 8: Sensitivity of the WT and mutants to photoinhibition. (A) Residual rates of oxygen evolution measured following photoinhibitory light treatment of thylakoids isolated from the WT (open circles), D2-Q129L (closed circles), and D2-Q129H (semiclosed circles) strains. The values are presented as a percentage of the rate obtained at 0 min treatment. (B) Growth characteristics of the WT, D2-Q129L, and D2-Q129H mutants on high salt (photoautotrophic) media. The WT and mutants were plated at the same cell densities and grown for a period of 2 weeks at a light intensity of ~500 μE m^{-2} s^{-1}.

of PQ in the Q_B site that has been studied using thermoluminescence in cyanobacteria and higher plants (reviewed in ref *42*). The TL yield and peak temperature of the B band under stress conditions is reduced relative to that measured under optimal conditions. This reduction in TL yield has been ascribed to an enhanced dissipation of excess excitation energy within the PSII RC via nonradiative charge recombination mechanisms which reduce $^3P_{680}$-mediated photooxidative damage to PSII. In the D2-Q129 mutants, the decrease in redox gap between Q_A and Q_B and increased probability of $S_2Q_B^-$ charge recombination were not accompanied by a concomitant decrease in TL yield, suggesting that nonradiative charge recombination pathways were not enhanced. Thus, the probability of forming $^3P_{680}$ by repopulating the $P_{680}^+Pheo_{D1}^-$ charge pair in the D2-Q129 mutants would be expected to increase. To determine whether the D2-Q129 mutants were more or less susceptible to photooxidative damage, we subjected WT and D2-Q129 mutant thylakoids to PI light and measured the subsequent decrease in oxygen evolving activity over time. It was observed that the D2-Q129L and D2-Q129H mutants had increased susceptibility to high light induced damage as was evident from the more rapid decline in oxygen evolving activity of the D2-Q129 mutant thylakoids when compared to WT (Figure 8A).

Further, in order to determine whether the increased susceptibility of the D2-Q129 mutants to photoinhibition had an effect on photoautotrophic growth under high light conditions, WT and D2-Q129 mutant cells were spotted on HS agar plates at equal cell densities and grown under 500 μmol photons m^{-2} s^{-1} of white light for two weeks. A slight retardation in growth and increased yellowing of the D2-Q129L and D2-Q129H cultures was observed relative to WT (Figure 8B). This effect on growth in the D2-Q129 mutants was presumably due to an increase in photooxidative damage relative to WT.

DISCUSSION

In this work we explored the effects of replacing D2-Q129, a highly conserved inactive branch acceptor side residue, with a nonconservative amino acid leucine (D2-Q129L) or a conservative amino acid histidine (D2-Q129H) in *C. reinhardtii*. Unlike its active branch counterpart D1-E130, which hydrogen bonds to $Pheo_{D1}$, the D2-Q129 residue is further away from the headgroup of $Pheo_{D2}$ and hence is unlikely to serve as a hydrogen bond donor.

Effect of D2-Q129 Mutagenesis on the Energetics of Charge Stabilization at the Acceptor Side of PSII. The flash-induced Chl fluorescence decay kinetics measured in the absence of DCMU showed significant differences between the WT and D2-Q129 mutants (Figure 3A). Three lifetime components (fast, intermediate, and slow) were used to fit the Chl fluorescence decay curves measured in the absence of DCMU. While the lifetimes of the fast and intermediate components indicative of forward ET in PSII were unchanged in the D2-Q129 mutants relative to WT, their relative contribution to the overall fluorescence decay was decreased. The lifetime of the slow component that arises due to $S_2Q_B^-$ charge recombination was accelerated 4−6-fold in the D2-Q129 mutants, indicative of a decrease in the overall stability of the $S_2Q_B^-$ state and a higher rate of reverse ET from $Q_AQ_B^-$ to $Q_A^-Q_B$. Further, the relative contribution of $S_2Q_B^-$ charge recombination to the decay of Chl fluorescence had an ~2.5-fold larger relative amplitude compared to WT which could be ascribed to a lower value for the equilibrium constant for ET from Q_A to Q_B or to weaker binding of plastoquinone to the Q_B site. Since the lifetime of the intermediate fluorescence decay lifetime component, indicative of plastoquinone binding in the Q_B site, did not change in the D2-Q129 mutants, we can assume that the change in the amplitude of this component was due to a lower equilibrium constant for Q_A to Q_B ET. A similar effect was seen in the D1-E130L/D2-Q129L double mutant in which the relative amplitude of $S_2Q_B^-$ charge recombination was also increased from 48% in D1-E130L to 58% in the D1-E130L/D2-Q129L double mutant. In the presence of DCMU, no differences were observed in the overall decay kinetics between WT and the D2-Q129L and D2-Q129H mutants or between the D1-E130L and D1-E130L/D2-Q129L mutants (Figure 3B, Table 2). These results indicate involvement of Q_B in the changes observed in the Chl fluorescence decay kinetics in the absence of DCMU.

TL arises from the radiative recombination of charge transfer pairs that recombine in a temperature-dependent manner. The peak temperature of a TL band reflects the energy stored in the charge transfer pair, which in turn is dependent on the redox potentials of the individual recombination partners assuming no change in distance or reorganization energy. As discussed earlier, TL that arises from the recombination of the S_2 state of the OEC on the donor side with the reduced states Q_A^- and Q_B^- leads to the formation of the Q-band and B band, respectively. The D2-Q129 mutation induced changes in the peak temperature of only the B band and not the Q-band (Figures 5, 6, and 7). Consistent with results from Chl fluorescence decay measurements, TL data from D2-Q129 mutants indicate that mutagenesis of the

D2-Q129 residue alters the redox properties of Q_B. Given that the D2-Q129 residue is located close to $Pheo_{D2}$, we wanted to unambiguously determine whether or not any of the inactive branch cofactors were involved in the charge recombination of Q_B^- with S_2 in the D2-Q129 mutants. To address this question, we generated the D1-E130L/D2-Q129L double mutant in both the active and inactive PSII RC cofactor branches. Our data clearly show that the D1-E130L/D2-Q129L double mutant manifests the combined effects of the two single mutations indicating that the acceleration of charge recombination from Q_B^- to the S_2 state of the water oxidation complex induced by the D2-Q129 mutation involves only the active branch and not inactive branch cofactors.

To ensure that the major TL band observed in the D2-Q129L, D2-Q129H, and D1-E130L/D2-Q129L mutants in the absence of Q_B site inhibitors was due to $S_2Q_B^-$ and not $S_2Q_A^-$ recombination, we treated the cells with PBQ prior to the measurements to oxidize the plastoquinone pool and minimize the contribution of reduced Q_A to the TL signal. The origin of the predominant TL bands observed in the WT and mutant cells in the absence of ET inhibitors after PBQ treatment was attributed to $S_2/_3Q_B^-$ recombination. Again, decreased B band peak temperatures were obtained in D2-Q129L and D2-Q129H mutants relative to WT and in the D1-E130L/D2-Q129L double mutant relative to D1-E130L, indicating a decrease in the stability of Q_B^- induced by D2-Q129 mutagenesis (Figure 7A,B).

Mutagenesis of D2-Q129 Lowers the Redox Potential of Q_B and the Driving Force for Q_A to Q_B ET. The driving force for forward ET is dependent on the energetic gap between Q_A and Q_B, which may be estimated from the ratio of the lifetimes of the slow component measured in the absence and presence of a Q_B site inhibitor, DCMU. This yields a redox gap of ~65 mV between Q_A and Q_B in WT in accordance with previous estimations (*43*, *44*). We calculate that the redox gap between Q_A and Q_B decreased to ~22 and ~25 mV in the D2-Q129L and D2-Q129H mutants, respectively. Since $S_2Q_A^-$ charge recombination and Q_A redox properties were not affected by D2-Q129 mutagenesis, we can conclude that the decrease in redox gap between Q_A and Q_B in the D2-Q129 mutants occurred due to a lowering of the Q_B/Q_B^- redox potential by ~40−45 mV, bringing it closer to the midpoint potential of the Q_A/Q_A^- couple. This decrease in Q_B redox potential causes a destabilization of Q_B^- and of the $S_2Q_B^-$ charge-separated state and is responsible for shifting the $Q_A^-Q_B \leftrightarrow Q_AQ_B^-$ equilibrium toward Q_A^- in the D2-Q129 mutants.

Evidence for a shift in the $Q_A^-Q_B \leftrightarrow Q_AQ_B^-$ equilibrium was also obtained from the results of Chl fluorescence induction kinetics measured under steady-state illumination which indicated that D2-Q129 mutagenesis results in an increase in the amplitude of the I phase, which is correlated with the formation/presence of Q_A^- (Figure 4). This phenotype has been observed before in *Chlamydomonas* D1-R257E and D1-R257M mutants, in which a large fraction of Q_A^- persists after flash excitation, indicative of an altered equilibrium constant of the reaction $Q_A^-Q_B \leftrightarrow Q_AQ_B^-$, in the direction of Q_A^- (*32*). Since substitutions of the D2-Q129 residue by amino acids with either conservative biochemical properties or otherwise shift the $Q_A^-Q_B \leftrightarrow Q_AQ_B^-$ equilibrium toward $Q_A^-Q_B$, mutagenesis of the D2-Q129 residue likely induces a structural change that alters Q_B site properties.

Position of D2-Q129 Relative to the Q_B Binding Site. Based on the sequence analogy between the D1 and D2 RC proteins, it would be expected that the D2-Q129 residue interacts with or hydrogen bonds to $Pheo_{D2}$. However, the side chain of the D2-Q129 residue is 3.9 Å away from the $Pheo_{D2}$ headgroup and is presumably too distant to serve as a hydrogen bond donor. The D2-Q129 residue side chain is located 3.03 Å away from the OH group of the D1-Y254 residue on the D1-*de helix*. The D1-*de helix* is situated between the fourth and fifth transmembrane helices of the D1 protein and has been shown to interact with Q_B and its competitive inhibitors (Figure 1) (*45*, *46*). Backbone-dependent *in silico* mutagenesis of D2-Q129 using PyMOL (DeLano Scientific LLC, San Carlos, CA) revealed that the predicted distance between the side-chain of D2-Q129 and the OH group of D1-Y254 decreased from 3.03 Å in WT to 1.03 and 0.67 Å in the D2-Q129H and D2-Q129L mutants, respectively. This suggests that the predicted decrease in distance between the mutagenized D2-Q129 side chain and the D1-*de helix* residue D1-Y254 could potentially impact the structure of the D1-*de helix* and the Q_B site, thereby altering the redox properties of Q_B.

Mutagenesis of residues located in the *de helix* of the D1 protein as in the D1-Y254S and D1-F255W mutants have been shown to lead to a decrease in stabilization of Q_B^- as observed by decreased B band peak temperatures obtained in TL measurements of these mutants (*47*). Moreover, a study in which combinatorial mutagenesis was applied to a highly conserved portion of the D1-*de helix* demonstrated that while many different combinations of amino acids in positions 254 to 257 of the D1 protein produced functional PSII RCs, all of the mutants had altered $Q_A^-Q_B \leftrightarrow Q_AQ_B^-$ equilibrium and Q_B/Q_B^- midpoint potentials relative to WT (*46*). More evidence for the involvement of the D1-*de helix* in determining Q_B redox potential comes from the site-directed mutagenesis of the highly conserved residue D1-R257 located at the C-terminal end of the D1-*de helix*. Although the side chain of D1-R257 points away from the Q_B binding pocket, site-directed mutagenesis to E, K, or Q causes a lowering of Q_B redox potential as evidenced from the lower B band peak temperatures in the mutants relative to WT (*38*). Overall, our results indicate that mutagenesis of the "inactive branch" residue D2-Q129 alters the redox potential of Q_B presumably by altered structural interactions of the D1-*de helix* with Q_B.

Mutations of D2-Q129 Increase Susceptibility to Photoinhibition. Although D2-Q129 mutagenesis had no significant effects on photoautotrophic growth under low light intensities, photoautotrophic growth under high light was impaired in the mutants relative to WT (Figures 2 and 8B). These results were consistent with those obtained from photoinhibitory light treatments of mutant thylakoids (Figure 8A). The increased sensitivity of the D2-Q129 mutants to high light may be explained by the increased yield of $S_2Q_B^-$ charge recombination relative to WT (Table 2). It is known that charge recombination reactions in PSII lead to oxidative damage via the triplet Chl-mediated formation of reactive oxygen species (*40*).

CONCLUSIONS

In this study, we have characterized the effects of mutagenizing the highly conserved inactive branch PSII residue, D2-Q129, on PSII electron transfer and stability of the charge-separated state. Mutagenesis of D2-Q129 to biochemically conservative (histidine) or nonconservative (leucine) amino acid residues results in (1) a decrease in the activation energy for charge recombination of Q_B^- with S_2, due to the lowering of the redox potential of Q_B, (2) no significant impact on the redox potential of Q_A or the donor side components, (3) a shift in the equilibrium constant for the reaction $Q_A^-Q_B \leftrightarrow Q_AQ_B^-$ toward Q_A^-, and (4) increased susceptibility to photoinhibitory light. This study provides insight into the extent of asymmetry between the two ET branches of PSII where analogous

active and inactive branch mutations can influence nonanalogous cofactors of the two branches. Our experimental data elucidate further the impact of individual "inactive" branch residues on PSII function. Our results also provide the first report of a single amino acid substitution of the D2 protein that affects the redox properties of Q_B.

REFERENCES

1. Zouni, A., Witt, H.-T., Kern, J., Fromme, P., Krauss, N., Saenger, W., and Orth, P. (2001) Crystal structure of photosystem II from *Synechococcus elongatus* at 3.8 Å resolution. *Nature 409*, 739–743.
2. Ferreira, K. N., Iverson, T. M., Maghlaoui, K., Barber, J., and Iwata, S. (2004) Architecture of the photosynthetic oxygen-evolving center. *Science 303*, 1831–1838.
3. Loll, B., Kern, J., Saenger, W., Zouni, A., and Biesiadka, J. (2005) Towards complete cofactor arrangement in the 3.0 Å resolution structure of photosystem II. *Nature 438*, 1040–1044.
4. Guskov, A., Kern, J., Gabdulkhakov, A., Broser, M., Zouni, A., and Saenger, W. (2009) Cyanobacterial photosystem II at 2.9-Å resolution and the role of quinones, lipids, channels and chloride. *Nat. Struct. Mol. Biol. 16*, 334–342.
5. Klimov, V. V., Klevanik, A. V., Shuvalov, V. A., and Krasnovsky, A. A. (1977) Reduction of pheophytin in the primary light reaction of photosystem II. *FEBS Lett. 82*, 183–186.
6. Klimov, V. V., and Krasnovsky, A. A. (1981) Pheophytin as the primary electron acceptor in photosystem 2 reaction centers. *Photosynthetica 15*, 592–609.
7. Dorlet, P., Xiong, L., Sayre, R. T., and Un, S. (2001) High field EPR study of the pheophytin anion radical in wild type and D1-E130 mutants of photosystem II in *Chlamydomonas reinhardtii*. *J. Biol. Chem. 276*, 22313–22316.
8. Klimov, V. V. (2003) Discovery of pheophytin function in the photosynthetic energy conversion as the primary electron acceptor of photosystem II. *Photosynth. Res. 76*, 247–253.
9. Groot, M. L., Pawlowicz, N. P., van Wilderen, L. J. G. W., Breton, J., van Stokkum, I. H. M., and van Grondelle, R. (2005) Initial electron donor and acceptor in isolated photosystem II reaction centers identified with femtosecond mid-IR spectroscopy. *Proc. Natl. Acad. Sci. U.S.A. 102*, 13087–13092.
10. Rappaport, F., Cuni, A., Xiong, L., Sayre, R., and Lavergne, J. (2005) Charge recombination and thermoluminescence in photosystem II. *Biophys. J. 88*, 1948–1958.
11. Holzwarth, A. R., Müller, M. G., Reus, M., Nowaczyk, M., Sander, J., and Rögner, M. (2006) Kinetics and mechanism of electron transfer in intact photosystem II and in the isolated reaction center: pheophytin is the primary electron acceptor. *Proc. Natl. Acad. Sci. U.S.A. 103*, 6895–6900.
12. Merry, S. A. P., Nixon, P. J., Barter, L. M. C., Schilstra, M., Porter, G., Barber, J., Durrant, J. R., and Klug, D. R. (1998) Modulation of quantum yield of primary radical pair formation in photosystem II by site-directed mutagenesis affecting radical cations and anions. *Biochemistry 37*, 17439–17447.
13. Cuni, A., Xiong, L., Sayre, R., Rappaport, F., and Lavergne, J. (2004) Modification of the pheophytin midpoint potential in photosystem II: modulation of the quantum yield of charge separation and of charge recombination pathways. *Phys. Chem. Chem. Phys. 6*, 4825–4831.
14. Cser, K., and Vass, I. (2007) Radiative and non-radiative charge recombination pathways in photosystem II studied by thermoluminescence and chlorophyll fluorescence in the cyanobacterium *Synechocystis* 6803. *Biochim. Biophys. Acta 1767*, 233–243.
15. Germano, M., Shkuropatov, A. Y., Permentier, H., de Wijn, R., Hoff, A. J., Shuvalov, V. A., and van Gorkom, H. J. (2001) Pigment organization and their interactions in reaction centers of photosystem II: optical spectroscopy at 6 K of reaction centers with modified pheophytin composition. *Biochemistry 40*, 11472–11482.
16. Xiong, L., Seibert, M., Gusev, A. V., Wasielewski, M. R., Hemann, C., Hille, C. R., and Sayre, R. T. (2004) Substitution of a chlorophyll into the inactive branch pheophytin-binding site impairs charge separation in photosystem II. *J. Phys. Chem. B 108*, 16904–16911.
17. Xiong, J., Subramaniam, S., and Govindjee (1996) Modeling of the D1/D2 proteins and cofactors of the photosystem II reaction center: implications for herbicide and bicarbonate binding. *Protein Sci. 5*, 2054–2073.
18. Kern, J., and Renger, G. (2007) Photosystem II: structure and mechanism of the water:plastoquinone oxidoreductase. *Photosynth. Res. 94*, 183–202.
19. Deisenhofer, J., and Michel, H. (1989) The photosynthetic reaction center from the purple bacterium *Rhodopseudomonas viridis*. *Science 245*, 1463–1473.
20. Minagawa, J., and Crofts, A. R. (1994) A robust protocol for site-directed mutagenesis of the D1 protein in *Chlamydomonas reinhardtii*: a PCR-spliced *psbA* gene in a plasmid conferring spectinomycin resistance was introduced into a psbA deletion strain. *Photosynth. Res. 42*, 121–131.
21. Goldschmidt-Clermont, M. (1991) Transgenic expression of aminoglycoside adenine transferase in the chloroplast: a selectable marker for site-directed transformation of chlamydomonas. *Nucleic Acids Res. 19*, 4083–4089.
22. Minai, L., Wostrikoff, K., Wollman, F.-A., and Choquet, Y. (2006) Chloroplast biogenesis of photosystem II cores involves a series of assembly-controlled steps that regulate translation. *Plant Cell 18*, 159–175.
23. Harris, E. H. (1989) The Chlamydomonas Sourcebook: A Comprehensive Guide to Biology and Laboratory Use, Academic Press, San Diego.
24. Cao, M., Fu, Y., Guo, Y., and Pan, J. (2009) *Chlamydomonas* (Chlorophyceae) colony PCR. *Protoplasma 235*, 107–110.
25. Sueoka, N. (1960) Mitotic replication of deoxyribonucleic acid in *Chlamydomonas reinhardi*. *Proc. Natl. Acad. Sci. U.S.A. 46*, 83–91.
26. Roffey, R. A., Kramer, D. A., Govindjee, and Sayre, R. T. (1994) Lumenal side histidine mutations in the D1 protein of photosystem II affect donor side electron transfer in *Chlamydomonas reinhardtii*. *Biochim. Biophys. Acta 1185*, 257–270.
27. Vass, I., Kirilovsky, D., and Etienne, A.-L. (1999) UV-B radiation-induced donor- and acceptor-side modifications of photosystem II in the cyanobacterium *Synechocystis* sp. PCC 6803. *Biochemistry 38*, 12786–12794.
28. Rutherford, W., Govindjee, and Inoue, Y. (1984) Charge accumulation and photochemistry in leaves studied by thermoluminescence and delayed light emission. *Proc. Natl. Acad. Sci. U.S.A. 81*, 1107–1111.
29. Govindjee (1995) Sixty-three years since Kautsky: chlorophyll *a* fluorescence. *Aust. J. Plant Physiol. 22*, 131–160.
30. Srivastava, A., Strasser, R. J., and Govindjee (1995) Polyphasic rise of chlorophyll *a* fluorescence in herbicide-resistant D1 mutants of *Chlamydomonas reinhardtii*. *Photosynth. Res. 43*, 131–141.
31. Strasser, R. J., Srivastava, A., and Govindjee (1995) Polyphasic chlorophyll *a* fluorescent transient in plants and cyanobacteria. *Photochem. Photobiol. 61*, 32–42.
32. Xiong, J., Minagawa, J., Crofts, A., and Govindjee (1998) Loss of inhibition by formate in newly constructed photosystem II D1 mutants, D1-R257E and D1-R257M, of *Chlamydomonas reinhardtii*. *Biochim. Biophys. Acta 1365*, 473–491.
33. Inoue, Y. (1996) Photosynthetic Thermoluminescence as a Simple Probe of Photosystem II Electron Transport, in Biophysical Techniques in Photosynthesis (Amesz, J., and Hoff, A. J., Eds.) pp 93–107, Kluwer Academic, The Netherlands.
34. Vass, I. (2003) The history of photosynthetic thermoluminescence. *Photosynth. Res. 76*, 303–318.
35. Ducruet, J.-M., and Vass, I (2009) Thermoluminescence: experimental. *Photosynth. Res. 101*, 195–204.
36. Rutherford, A. W., Crofts, A. R., and Inoue, Y. (1982) Thermoluminescence as a probe of photosystem II photochemistry. The origin of the flash-induced glow peaks. *Biochim. Biophys. Acta 682*, 457 465.
37. Velthuys, B. R., and Amesz, J. (1974) Charge accumulation at the reducing side of system 2 of photosynthesis. *Biochim. Biophys. Acta 333*, 85–94.
38. Rose, S., Minagawa, J., Seufferheld, M., Padden, S., Svensson, B., Kolling, D. R. J., Crofts, A. R., and Govindjee (2008) D1-arginine mutants (R257E, K, and Q) of *Chlamydomonas reinhardtii* have a lowered Q_B redox potential: analysis of thermoluminescence and fluorescence measurements. *Photosynth. Res. 98*, 449–468.
39. Ducruet, J.-M. (2003) Chlorophyll thermoluminescence of leaf discs: simple instruments and progress in signal interpretation open the way to new ecophysiological indicators. *J. Exp. Bot. 54*, 2419–2430.
40. Krieger-Liszkay, A., Fufezan, C., and Trebst, A. (2008) Singlet oxygen production in photosystem II and related photoprotection mechanism. *Photosyn. Res. 98*, 551–564.
41. Vass, I., and Cser, K. (2009) Janus-faced charge recombinations in photosystem II photoinhibition. *Trends Plant Sci. 14*, 200–205.
42. Ivanov, A. G., Sane, P. V., Hurry, V., Öquist, G., and Huner, N. P. A. (2008) Photosystem II reaction center quenching: mechanisms and physiological role. *Photosynth. Res. 98*, 565–574.

43. Robinson, H. H., and Crofts, A. R. (1983) Kinetics of the oxidation-reduction reactions of the photosystem II quinone acceptor complex, and the pathway for deactivation. *FEBS Lett. 153*, 221–226.
44. Cser, K., Deák, Z., Telfer, A., Barber, J., and Vass, I. (2008) Energetics of photosystem II charge recombination in *Acaryochloris marina* studied by thermoluminescence and flash-induced chlorophyll fluorescence measurements. *Photosynth. Res. 98*, 131–140.
45. Trebst, A. (1987) The three dimensional structure of the herbicide binding niche on the reaction center polypeptides of photosystem II. *Z. Naturforsch. 42c*, 742–750.
46. Kless, H., and Vermaas, W. (1995) Many combinations of the amino acid sequences in a conserved region of the D1 protein satisfy photosystem II function. *J. Mol. Biol. 246*, 120–131.
47. Ohad, N., and Hirschberg, J. (1992) Mutations in the D1 subunit of photosystem II distinguish between quinone and herbicide binding sites. *Plant Cell 4*, 273–282.